Numerical study on ergodic properties of triangular billiards

Roberto Artuso,[1,2] Giulio Casati,[1,2] and Italo Guarneri[1,3]
[1]*Istituto di Scienze Matematiche, Fisiche e Chimiche, Via Lucini 3, I-22100 Como, Italy*
[2]*Istituto Nazionale di Fisica della Materia, Unità di Milano and INFN, Sezione di Milano, Italy*
[3]*Istituto Nazionale di Fisica della Materia, Unità di Milano and INFN, Sezione di Pavia, Italy*
(Received 16 September 1996)

We consider the motion of a point particle in right triangular billiards. By considering the global dynamics (when acute angles are not rationally connected to π), or the discrete reduced dynamics (when acute angles are rational multiples of π), we find numerical evidence for the conjecture that the motion is ergodic and weakly mixing. These dynamical features are intimately related to nontrivial scaling properties of the spectrum of the evolution operator. [S1063-651X(97)12703-9]

PACS number(s): 05.45.+b

I. INTRODUCTION

We consider the motion of a point particle, with unity velocity, inside a right triangular billiard. This is equivalent [1] to the motion of two point particles on the unit interval, interacting only through elastic collisions, their mass ratio inducing the angle α of the corresponding triangle via the relation $\alpha=\arctan\sqrt{m_1/m_2}$.

The way to look at the dynamics on these triangular billiards depends essentially on whether or not α is rationally connected to π. As a matter of fact we can associate a group to each triangle according to the following construction: denote by $\sigma_1,\sigma_2,\sigma_3$ the reflections about the lines ℓ_1,ℓ_2,ℓ_3 (factoring away translations by considering reflections of points on a circle) defined by the triangle's sides; Then W_Δ will be the subgroup generated by $\{\sigma_i\}$, $i=1,2,3$. When α is rationally connected to π, the subgroup W_Δ is finite, and coincides with D_N, the dihedral group corresponding to the angle π/N, where N is the least common multiple of n_1,n_2,n_3 defined by vertex angles being $\pi m_i/n_i$. Thus, when α is rationally connected to π, the phase space is split into invariant manifolds R_θ, $\theta\in[0,\pi/N]$, individuated by the initial angle (the finite $2N$ set of possible angles is connected to the initial one via operations of D_N). Thus rational triangles are obviously nonergodic: the interest is anyway cast into dynamical properties of the flow restricted to the invariant surfaces R_θ (directional dynamics). The topology of these invariant surfaces is dictated by the nature of vertex angles: it can be shown (see, for instance, [2]) that the genus of the surface is given by

$$g=1+\frac{N}{2}\sum_{i=1}^{3}\frac{m_i-1}{n_i}, \tag{1}$$

where $\pi m_i/n_i$ are indeed the vertex angles. We notice that the invariant surfaces will be tori only when all $m_i=1$: this means that, in the present case, the only integrable cases correspond to $\alpha=\pi/4,\ \pi/3,\ \pi/6$.

Together with the continuous time flow, it is possible to introduce the Birkhoff-Poincaré map, using the coordinates s,ϕ, where s is the position along the perimeter and $\phi\in[-\pi/2,\ \pi/2]$ is the outgoing angle with respect to the normal in s. When we consider flows in a rational triangle, we remarked above that we have a finite set of $2N$ possible angles: for each side this corresponds to N possible outgoing angles, and thus, by considering N replicas of the sides the mapping becomes one dimensional. Once we normalize by the total length

$$m_\theta=\sum_{i=1}^{3} l_i(\sin\phi_{i,1}+\sin\phi_{i,2}+\ \cdot\ \cdot\ \cdot+\sin\phi_{i_N}),$$

where $\phi_{i,k}$, $k=1,\ldots,N$, are the possible outgoing angles from the ith side (whose length is l_i), we obtain a map of the unit interval into itself, characterized by remarkable properties: in fact it is an (orientation reversing) interval exchanging transformation (see, for example, [1] for more details on this feature, and further references are contained in [2,3]).

A few facts are rigorously known about ergodic properties of triangle billiards (or, more generally, for motion in polygonal billiards): we follow closely [2,3]: (i) The set of ergodic triangles is a dense G_δ (intersection of a countable number of dense open sets) in a suitable topology [4]. (ii) The directional dynamics in a rational triangle is ergodic in almost all directions with respect to the Lebesgue measure [4]. (iii) The directional dynamics in a rational triangle is not mixing for any direction [5]. We also quote from [3]: ''A prevailing opinion in the mathematical community is that polygonal billiards are never mixing, but this has not been established. On the other hand, it seems plausible that there are weakly mixing polygons, but this also remains an open question.'' As a matter of fact a theorem, which, however, does not directly apply to triangles, establishing that weak mixing is a G_δ generic property in a particular class of polygonal billiards, has been proved in [6]. We recall (see, for example, [1]) that a dynamical system is weakly mixing if for any L^2 pair of observables,

$$\lim_{t\to\infty}\frac{1}{t}\int_0^t d\tau\left[\int_M d\mu(x)f(T^\tau x)g(x)-\int_M d\mu(x)f(x)\int_M d\mu(x)g(x)\right]^2=0 \tag{2}$$

that is integrated correlation functions decay to zero, while correlation functions themselves have the same property only

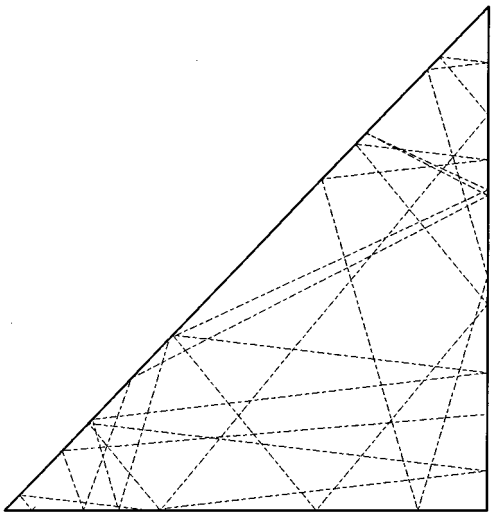

FIG. 1. A triangle billiard.

if the system is in effect mixing. Together with dynamic properties, such as weak mixing, we also want to investigate numerically spectral properties. We denote by

$$T^t = \int e^{2\pi i t\lambda} d\mathcal{E}(\lambda) \tag{3}$$

the spectral resolution of the evolution operator. Then, each $f \in L^2(M,\mu)$, orthogonal to 1, induces a spectral measure via $\langle \mathcal{E}(\lambda) f | f \rangle$. There are connections between spectral and dynamical properties: for instance (see, for example, [18]), if the set of measures just defined is absolutely continuous with respect to the Lebesgue measure then the system has to be mixing.

II. DYNAMICAL AND SPECTRAL QUANTITIES OBSERVED

We consider triangles such as the one in Fig. 1: α is the acute angle formed with the horizontal axis. The units are chosen in such a way that the point particle has unit velocity and the horizontal side has length one. The observable whose correlations we investigate is the horizontal component of the velocity v_x (which has zero average with respect to the invariant measure $d\mu = (1/2\pi A) dx\, dy\, d\theta$, where A denotes the area of the triangle. So we denote by $C(t)$ the (phase averaged) correlation function

$$C(t) = \int d\mu v_x T^t(v_x), \tag{4}$$

while the corresponding integrated correlation function is

$$C_{\text{int}}(t) = \frac{1}{t} \int_0^t d\tau |C(\tau)|^2. \tag{5}$$

We may also consider time-averaged correlation functions (which coincide with the former ones, when the system is ergodic)

$$C_{\text{time}}(t) = \lim_{\tau \to \infty} \frac{1}{\tau} \int_0^\tau d\varepsilon T^{t+\varepsilon}(v_x) T^{\varepsilon}(v_x). \tag{6}$$

Correlation functions may also be defined for the Birkhoff-Poincaré discrete dynamics: the invariant measure is in this case proportional to $ds \cos(\phi) d\phi$. In the former section we observed that the directional dynamics for rational cases leads to a map of the unit interval into itself (the orientation reversing interval exchange transformation): if we denote the normalized phase variable by z, and by J the mapping the correlation function we consider for this case will refer to $f(z) = \sin[\pi(z - 1/2)]$:

$$C_{dd}(n) = \int_0^1 dz f(z) f(J^n z). \tag{7}$$

In terms of the spectral resolution of the evolution operator, Eq. (4) may be rewritten as

$$C(t) = \int d\langle \mathcal{E}(\lambda) v_x | v_x \rangle e^{2\pi i t\lambda}, \tag{8}$$

and thus in principle the spectral measure may be recovered by the correlation series via Fourier inversion. In practice we have to be careful as we have a *finite* correlation sequence (moreover we have a discrete sampling of the continuous time): as motivated in [8,9] the best approach seems to be to perform the (approximated) inversion of Eq. (8) by using a triangular window [10]; this procedure guarantees also that the finite approximations to the spectral measure will be positive. Thus, each correlation sequence out to $T_{\max}$ time steps allows a reconstruction of the spectral measure down to a scale $\ell_k = (2T_{\max} + 1)^{-1}$ through

$$\wp_{m,\ell_k} = \frac{1}{2T_{\max} + 1} \sum_{j=-T_{\max}}^{T_{\max}} W_j C(t_j) e^{2\pi i t_j m/(2T_{\max}+1)}, \tag{9}$$

where the use of the triangular window implies $W_j = (T_{\max} - |t_j|)/T_{\max}$. A quantitative characterization of the scaling properties of the spectral measure is provided, for instance, by the set of generalized dimensions [11] D_q, which are defined in terms of the sums $\chi_k(q) = \Sigma_{j=1}^{N_k} \wp_{j,\ell_k}^q$ through

$$D_q = \lim_{k \to \infty} \frac{1}{q-1} \frac{\ln \chi_k(q)}{\ln \ell_k} \tag{10}$$

when $q \neq 1$. For $q = 1$ we have

$$D_1 = \lim_{k \to \infty} \frac{\sum_{j=1}^{N_k} \wp_{j,\ell_k} \ln \wp_{j,\ell_k}}{\ln \ell_k}. \tag{11}$$

These spectral exponents are related to dynamical properties: for instance, D_2, the so-called correlation dimension, rules the decay mode of the integrated correlation function [12,13]

$$C_{\text{int}}(t) \sim t^{-D_2}. \tag{12}$$

The information dimension is also related to growth properties in time of the moments of the probability distribution [14–17]. We describe how to get such moments for the discrete directional dynamics. Here we have a single phase variable z: its value at time n is determined by n and z_0 (the

initial value). The dependence on z_0 of a function of the phase variable z may be expressed through a Fourier representation

$$f(z(n,z_0))=\sum_{k=-\infty}^{\infty} c_k(n)e^{2\pi i z_0 k}. \tag{13}$$

We can thus define the moments

$$m^{(\beta)}(n)=\sum_{k=-\infty}^{\infty}|k|^{\beta}\frac{1}{n}\sum_{l=0}^{n-1}|c_k(l)|^2. \tag{14}$$

In particular we considered as phase function again, $f(z)=\sin[\pi(z-1/2)]$. As the mapping J is discontinuous, we are forced to consider moments with $\beta<1$, otherwise we get diverging quantities. If moments grow algebraically,

$$m^{(\beta)}(n)\sim n^{\varphi(\beta)}, \tag{15}$$

then [14–16] D_1 is a lower bound to $\varphi(\beta)/\beta$. This description originated in a quantum mechanical context, where these moments are connected to the spreading of an initially localized wave packet on a larger and larger number of basis elements.

III. NUMERICAL EXPERIMENTS

Irrational triangles

The first task is to check ergodicity: it is rather hard to exhibit this feature by just looking, for instance, at the Birkhoff-Poincaré return map, as there must be quite different time scales in the problem: this is essentially connected to the possibility of recovering any angle (modulo horizontal and vertical reflections) through α shifts. If we look at a phase portrait for longer and longer time, we perceive some sort of ''hierarchical'' filling of holes, which is presumably directly connected to number-theoretical properties of α: we give an example of the phase portrait for quite long time sequences in Fig. 2, where our choice for the variables is such that the invariant measure coincides with the Lebesgue measure.

A check on ergodicity was also performed in the quantities we want to study in some detail: the results support the expectation that motion in irrational triangles is ergodic. As an example consider Fig. 3, in which we compare the behavior of time averages and phase average for the autocorrelation function of the horizontal component of the velocity. Whenever we refer to phase averages we mean Monte Carlo integration (see, for example, [19]) over a set of $N_{\rm ph}$ initial conditions. The standard random number generator we use is based on a subtractive method (see Knuth [20] for details): in a variety of cases we checked that the use of a regular grid as initial conditions leads to the same results.

The next step involves a simultaneous analysis of $C(t)$ and $C_{\rm int}(t)$, as decay to zero of the phase averaged correlation function would not rule out mixing, while weak mixing (as a *maximal* property) would require convergence to zero of $C_{\rm int}(t)$, while the correlation function itself should not have a $t\mapsto\infty$ limit. A weak mixing property is supported numerically when we consider the vertex angle α connected to π through quadratic irrationals [in Figs. 4 and 5 we report

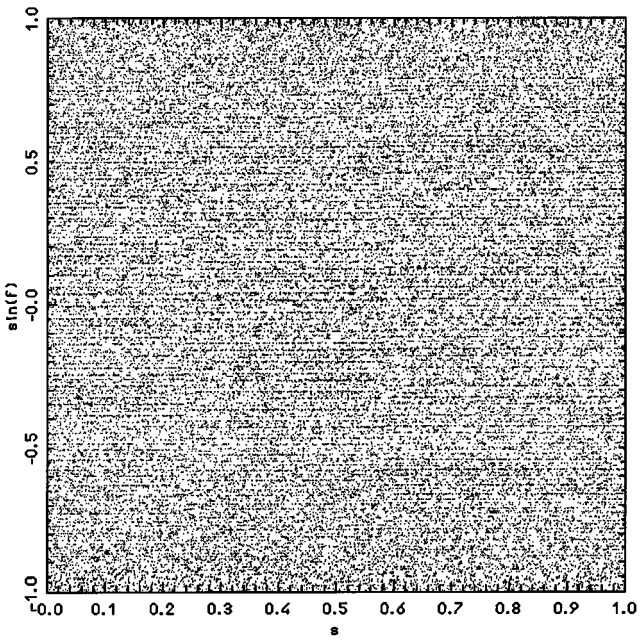

FIG. 2. Phase portrait of a single trajectory of $\alpha=\pi(\sqrt{5}-1)/4$ (discrete dynamics): the plot consists of 5×10^4 points, each obtained after 2×10^6 collisions from the former.

the results for $\alpha=\pi\sqrt{2}/4$, similar results hold for $\alpha=\pi(\sqrt{5}-1)/4$]. The integrated correlation function $C_{\rm int}(t)$ exhibits always a power-law decay to zero (cf. Fig. 4), with an exponent that is slightly smaller that 1. By looking at Fig. 5, we stress that a mixing property is not ruled out, as the correlation function itself seems to vanish asymptotically, albeit in a noisy way.

As explained in the former section we can reconstruct from the correlation sequence an approximation to the spec-

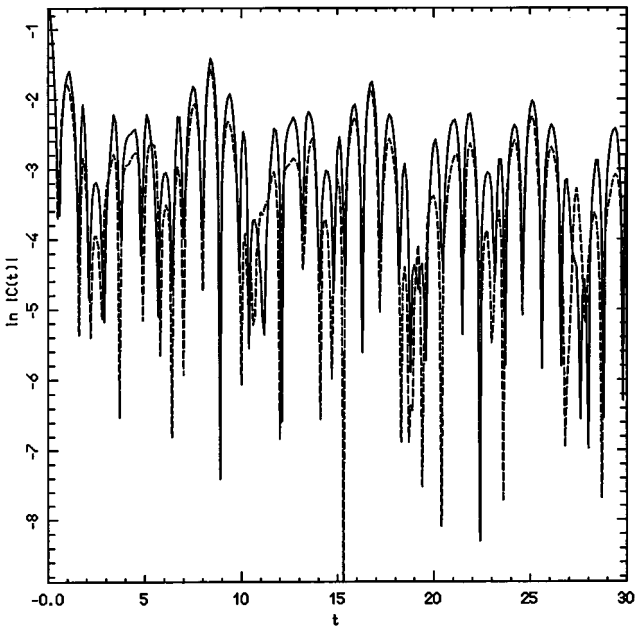

FIG. 3. $C(t)$ (full line) and $C_{\rm time}(t)$, for $\alpha=\pi(\sqrt{5}-1)/4$. Phase average refers to 2×10^5 initial conditions, while the time sequence giving $C_{\rm time}(t)$ is $T_{\rm max}=10^6$.

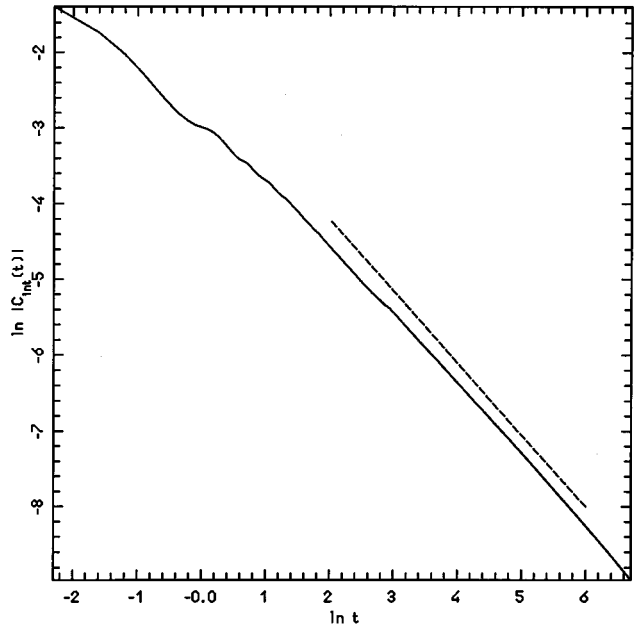

FIG. 4. $\ln C_{\rm int}(t)$ vs $\ln t$ for $\alpha=\pi\sqrt{2}/4$. The phase average refers to 2×10^7 points; the dashed straight line has a slope $-D_2\simeq0.95$.

tral measure: in particular this allows for a calculation of D_2, which, as remarked before, should coincide with the decay exponent. In Fig. 6 we plot finite order estimates of D_1 and D_2 for finer and finer scales (more and more correlation points). In Table I we compare decaying components γ [such as $C_{\rm int}(t)\sim t^{-\gamma}$] and D_2 [as reconstructed by Fourier inversion of $C(t)$] for a number of irrational values of α.

As regards the weak mixing conjecture, as a *maximal* ergodic property, the situation is not resolved by our investigations, in the sense that apparently also correlation functions tend to zero (and not only the integrated ones). This phenomenon does not seem to be related to number-

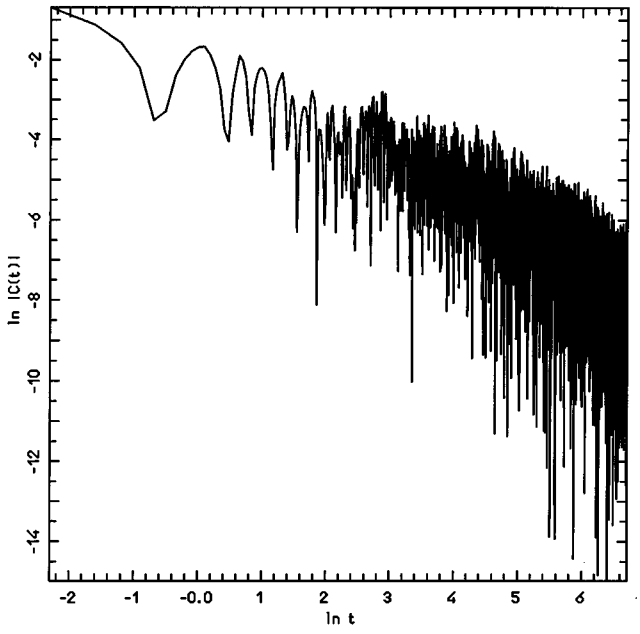

FIG. 5. $\ln|C(t)|$ vs $\ln t$ for the same case as Fig. 4.

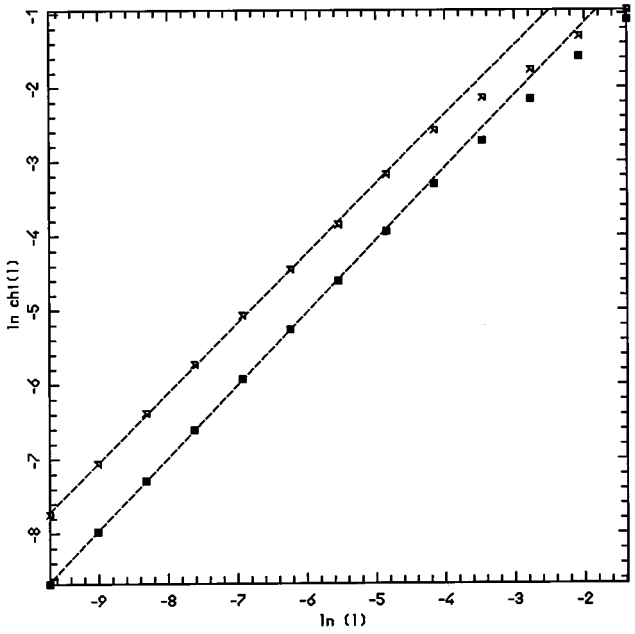

FIG. 6. $\ln\chi_k(2)$ vs $\ln\ell_k$ (upper symbols), and $\Sigma\wp_{i,k}\ln\wp_{i,k}$ vs $\ln\ell_k$ for the same case as Fig. 4. D_2 and D_1 are the asymptotic values of the respective slopes. The dashed lines are obtained through a least square fit over the last seven values.

theoretical properties of α, as we can see from Fig. 7, where α is a poor irrational multiple of π.

Rational triangles

Phase averages

We noted in the Introduction that whenever α is rationally connected to π the motion of the point particle is surely not ergodic (and the phase space is foliated by R_θ invariant surfaces determined by the initial value of the velocity vector and the group properties induced by α). Nevertheless, the decaying properties of phase averages (''microcanonical'' averages) are of some interest by themselves, even though it is *a priori* clear that they will not be connected to any time average. In particular, this point of view was originated some years ago in [7], where it was shown that (in some ''generic'' sense) phase averaged (on the energy surface) correlation functions for integrable systems are expected to decay to their limit value as $C(t)-C(\infty)\sim t^{(1-N)/2}$, where N is the number of degrees of freedom of the system. So we com-

TABLE I. γ, D_2, and D_1 for a number of irrational vertex angles. The errors on γ are determined by linear regression on exponentially sampled points on the integrated correlation functions. The errors on dimension come from linear regression over the last five data in sequences as in Fig. 6.

α	γ	D_2	D_1
$\pi(\sqrt{5}-1)/4$	0.90 ± 0.07	0.90 ± 0.05	0.97 ± 0.02
$\pi\sqrt{2}/4$	0.95 ± 0.02	0.95 ± 0.02	0.98 ± 0.01
$\pi e/8$	0.97 ± 0.01	0.95 ± 0.02	0.98 ± 0.01
$\pi^2/8$	0.97 ± 0.01	0.97 ± 0.02	0.99 ± 0.01
$\pi\sqrt{3}/4$	0.97 ± 0.01	0.97 ± 0.01	0.99 ± 0.005

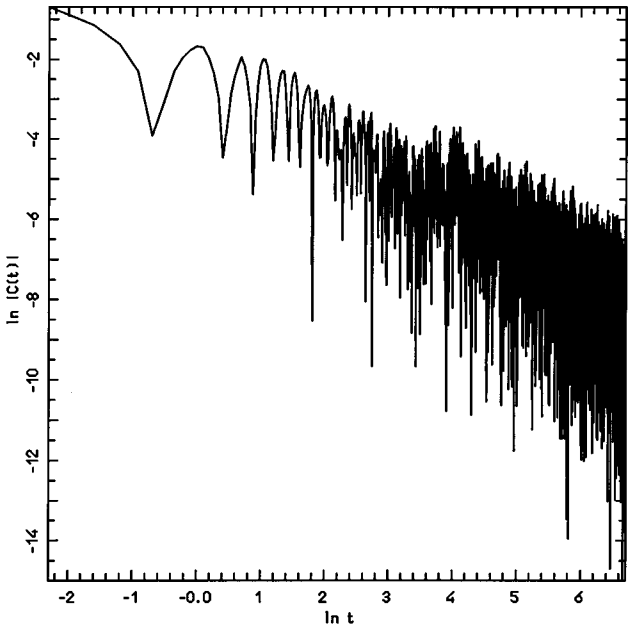

FIG. 7. $\ln|C(t)|$ vs $\ln t$ for $\alpha=\pi^2/8$. The phase average refers to 2×10^7 points.

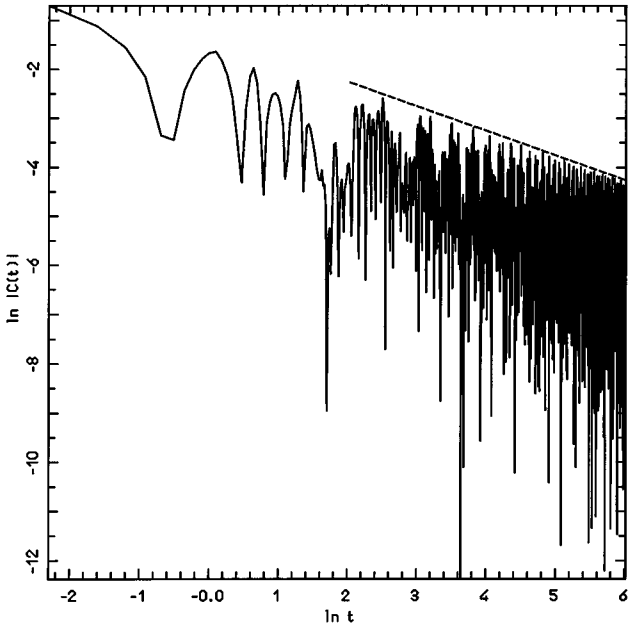

FIG. 9. $\ln|C(t)|$ vs $\ln t$ for the same case as Fig. 8; the dashed straight line has a slope $-\frac{1}{2}$.

puted microcanonical correlation functions for the integrable case $\alpha=\pi/3$: with our choice of observables $C(\infty)=0$ and the results are plotted in Figs. 8 and 9. Though the correlation function $C(t)$ has a quite complex behavior, which we did not analyze in detail, it seems to possess an envelope satisfying the law suggested in [7] (which for the present case predicts a $1/\sqrt{t}$ decay). In Fig. 8 we plot the behavior of the integrated correlation function, which again exhibits a power-law decay to zero, with an exponent $\gamma=0.89\pm0.01$. Again this coincides approximately with D_2 calculated via inverse Fourier transform of the correlation sequence: this procedure gives $D_2\simeq0.90$. We noted the Introduction that for generic rational values of α the system is not integrable, as invariant surfaces are topologically distinct from tori (and possess higher genus): we have preliminary indications that microcanonical averages in this case are qualitatively different from the integrable situations, and in particular a decaying upper envelope for $C(t)$ is no longer observed.

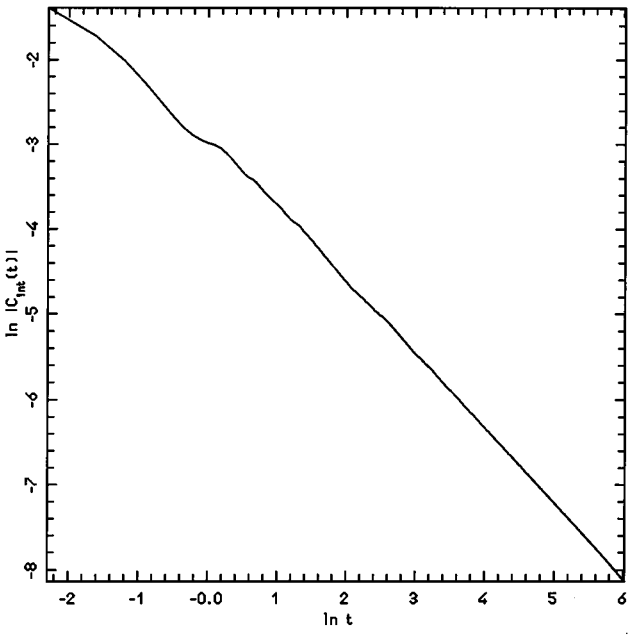

FIG. 8. $\ln C_{\rm int}(t)$ vs $\ln t$ for $\alpha=\pi/3$. Phase average refers to 10^7 initial conditions.

Directional dynamics

Here we leave the global phase space and investigate the motion on invariant surfaces R_θ, individuated by the fraction connecting α to π, and a choice of a direction in the full phase space (see the first section). As a specific example we investigated the case $\alpha=\pi/16$ (where the invariant surfaces have the topology of a sphere with four handles), fixing as phase space angle $\theta_0=1.873\,817\,640\,780\,35$. In this case we analyzed the dynamics in terms of the one-dimensional Birkhoff-Poincaré map, and thus compute $C_{dd}(n)$ and the corresponding integrated counterpart

$$C_{dd|\rm int}(n)=\frac{1}{n}\sum_{k=0}^{n-1}|C_{dd}(k)|^2. \tag{16}$$

The results are here fully consistent with weak mixing as *maximal* ergodic property, as $C_{dd}(n)$ is not converging to zero in our numerical simulation, while $C_{dd|\rm int}(n)$ vanishes according to a power law (see Figs. 10 and 11). Again the decay exponent is consistent with the correlation dimension (we have $\gamma=0.79\pm0.05$, while $D_2\simeq0.8$). Here we may also analyze the growth rate of moments, according to Eq. (15). An example is provided in Fig. 12, where we consider $m^{(1/3)}(n)$, which grows algebraically, with an exponent $\varphi(1/3)/(1/3)\simeq0.885$ (the information dimension—which bounds the normalized growth rate from below—is in this case $D_1\simeq0.88$.

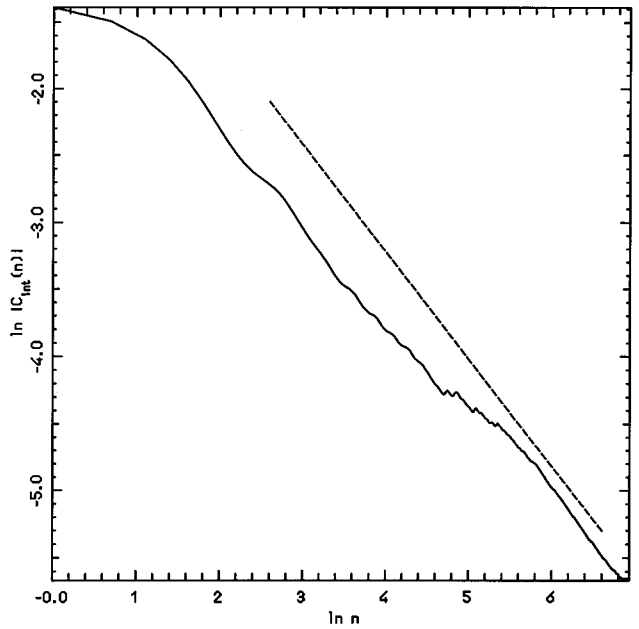

FIG. 10. $\ln C_{\mathrm{dd|int}}(n)$ vs $\ln n$ for $\alpha=\pi/16$, and the value of θ_0 reported in the text. We considered 2^{10} collisions, and averaged over 10^7 initial conditions; the dashed straight line has a slope $-D_2\simeq-0.8$.

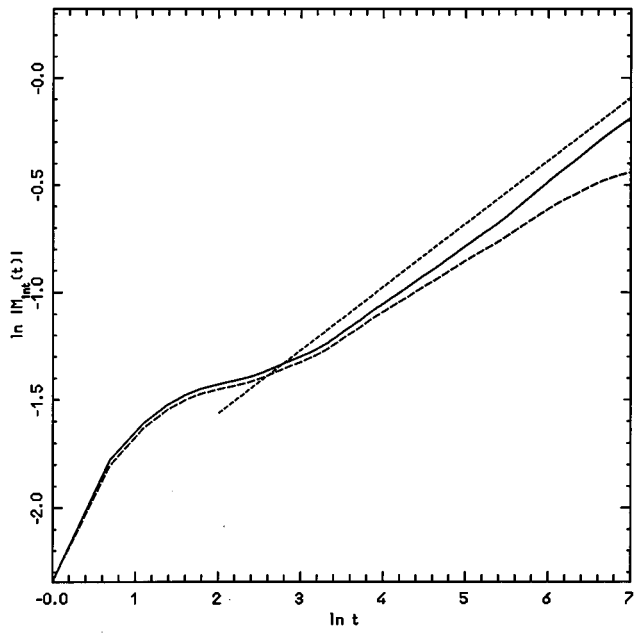

FIG. 12. $\ln m^{(1/3)}(n)$ vs $\ln n$ for the same case as Figs. 10 and 11. The dashed line was obtained by using a Fourier basis of 2^{12} elements, while the full line was obtained with a basis of 2^{17} elements. The dotted straight line has a slope $D_1/3\simeq0.89/3$.

As a last remark we present an investigation on $\alpha=\pi/10$, where different θ_0 are considered. From the behavior of $C_{dd|\mathrm{int}}(n)$ (see Fig. 13) it is clear that dynamical (and thus spectral) properties are highly sensitive to the choice of θ_0.

IV. CONCLUSIONS

We have performed a series of numerical investigations on right triangular billiards. Our purpose was to check whether the conjectures (or generic-nonconstructive results), based on remarkable mathematical analysis, are susceptible to be scrutinized by direct investigations. We have found evidences of ergodic and weakly mixing behavior for the global dynamics of ''irrational'' triangles, where, however, a mixing property is not ruled out. In the case of reduced discrete dynamics we have instead clear evidence of weak mixing as a maximal ergodic property.

In both cases weak mixing decay rates (as well as mo-

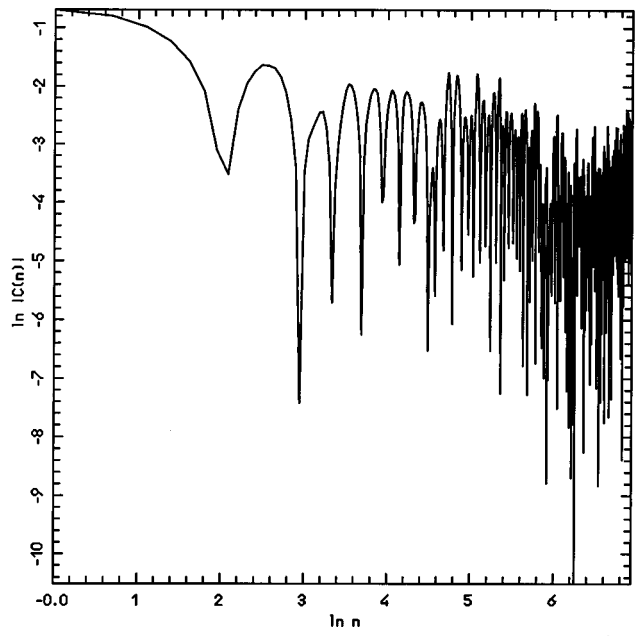

FIG. 11. $\ln|C_{dd}(n)|$ vs $\ln n$ for the same case as Fig. 10.

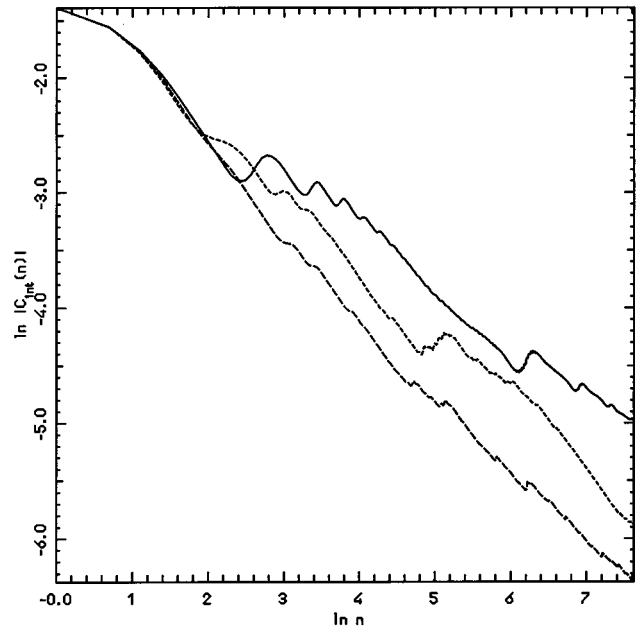

FIG. 13. $\ln C_{dd|\mathrm{int}}(n)$ vs $\ln n$ for $\alpha=\pi/10$: the full line refers to $\theta_0=1.873\,817\,640\,780$, the dashed line to $\theta_0=\sqrt{2}$, and the dotted line to $\theta_0=e/3$. Each curve is obtained by considering 2^{11} collisions, and a phase average over 10^7 initial conditions.

ments spreading for directional dynamics) are in agreement with exponents related to scaling properties of the spectral measure (namely, D_2 and D_1). Also microcanonical, nonergodic averages for rational triangles behave in accordance with theoretical expectations.

ACKNOWLEDGMENTS

R.A. thanks Mirko Degli Esposti for discussions and useful guidance through the mathematical literature on polygons.

[1] I. P. Kornfeld, S. V. Fomin, and Y. G. Sinai, *Ergodic Theory* (Springer, Berlin, 1982).
[2] E. Gutkin, Physica **19D**, 311 (1986).
[3] E. Gutkin, J. Stat. Phys. **83**, 7 (1996).
[4] S. Kerckhoff, H. Masur, and J. Smillie, Ann. Math. **124**, 293 (1986).
[5] A. Katok, Isr. J. Math. **35**, 301 (1980).
[6] E. Gutkin and A. Katok, in *Holomorphic Dynamics*, Lecture Notes in Mathematics Vol. 1345 (Springer, Berlin, 1989).
[7] G. Casati, F. Valz-Gris, and I. Guarneri, Physica **3D**, 644 (1981).
[8] M. Samuelides, R. Fleckinger, L. Touzillier, and J. Bellissard, Europhys. Lett. **1**, 203 (1986).
[9] R. Artuso, D. Belluzzo, and G. Casati, Europhys. Lett. **25**, 181 (1994).
[10] F. J. Harris Proc. IEEE **66**, 51 (1978).
[11] H. G. E. Hentschel and I. Procaccia, D Physica **8**, 435 (1983).
[12] R. Ketzmerick, G. Petschel, and T. Geisel, Phys. Rev. Lett. **69**, 695 (1992).
[13] M. Holschneider, Commun. Math. Phys. **160**, 457 (1994).
[14] I. Guarneri, J. Math. Phys. **37**, 5195 (1996).
[15] I. Guarneri, Europhys. Lett. **10**, 95 (1989); **21**, 729 (1993).
[16] I. Guarneri and G. Mantica, Ann. Inst. Henri Poincaré **61**, 369 (1994).
[17] A. S. Pikovsky, M. A. Zaks, U. Feudel, and J. Kurths, Phys. Rev. E **52**, 285 (1995).
[18] V. I. Arnold and A. Avez, *Ergodic Problems of Classical Mechanics* (Addison-Wesley, Redwood City, 1989).
[19] J. M. Hammersley and D. C. Handscomb, *Monte Carlo Methods* (Methuen, London, 1964).
[20] D. E. Knuth, *The Art of Computer Programming, Vol. II, Seminumerical Algorithms* (Addison-Wesley, Reading, MA, 1981).